scientific reports

Check for updates

OPEN

Machine learning aided UV absorbance spectroscopy for microbial contamination in cell therapy products

Shruthi Pandi Chelvam[1], Alice Jie Ying Ng[1], Jiayi Huang[1], Elizabeth Lee[1], Maciej Baranski[1], Derrick Yong[1,2,3], Rohan B. H. Williams[1,4], Stacy L. Springs[1,5] & Rajeev J. Ram[1,6]✉

We demonstrate the feasibility of machine-learning aided UV absorbance spectroscopy for in-process microbial contamination detection during cell therapy product (CTP) manufacturing. This method leverages a one-class support vector machine to analyse the absorbance spectra of cell cultures and predict if a sample is sterile or contaminated. This label-free technique provides a rapid output (< 30 minutes) with minimal sample preparation and volume (< 1 mL). Spiking of 7 microbial organisms into mesenchymal stromal cells supernatant aliquots from 6 commercial donors showed that contamination events could be detected at low inoculums of 10 CFUs with mean true positive and negative rates of 92.7% and 77.7% respectively. The true negative rate further improved to 92% after excluding samples from a single donor with anomalously high nicotinic acid. In cells spiked with 10 CFUs of *E. coli*, contamination was detected at the 21-hour timepoint, demonstrating comparable sensitivity to compendial USP < 71 > test (~ 24 hours). We hypothesize that spectral differences between nicotinic acid and nicotinamide in the UV region are the underlying mechanisms for contamination detection. This approach can be deployed as a preliminary test during different CTP manufacturing stages, for real-time, continuous culture monitoring enabling early detection of microbial contamination, assuring safety of CTP.

Advanced therapy medicinal products (ATMPs) are innovative medicines specifically designed to treat rare, severe and chronic diseases in which conventional treatment methods have proven to be inadequate. The field of ATMPs includes somatic-cell based therapies, stem-cell based therapies, gene and tissue-engineered therapies to repair damaged cells and tissues and to treat degenerative diseases[1]. These therapies involve manipulation of cells and tissues in vitro using nutrient rich stem cell cultures, which makes the process vulnerable to contamination by microbial species[2]. As current cell therapy product (CTP) manufacturing processes do not allow for terminal sterilization of products, there is a need for sterility testing of CTPs to ensure the safety of the product prior to infusion into patients[3]. With the field of ATMPs newly emerging, there are no sterility testing protocols specifically designed for the manufacturing and release of CTPs. Hence, the industry has adopted existing regulatory methods such as the United States Pharmacopeia (USP) chapter < 71 > as part of sterility testing to detect microbial contamination. The USP < 71 > was initially drafted for the release of large-batch pharmaceutical drugs which limits its suitability to the field of ATMPs[3].

With the lack of sterility test frameworks specific to ATMPs, the traditional USP < 71 > has been the gold standard for sterility testing of CTPs. These tests involve direct inoculation or membrane filtration methods, in specific growth mediums such as Tryptic Soy Broth (TSB) and Fluid Thioglycollate Medium (FTM) over an incubation period of up to 14 days[4]. Contamination is evaluated based on visual inspection for turbidity. The presence of turbidity triggers subcultures into secondary broths, with both original and subcultures incubated for at least additional 4 days[5]. However, turbidity may be misleading as cell culture media components and CTPs scatter light and contribute to turbidity, resulting in a sample being misinterpreted as contaminated[6].

[1]Critical Analytics for Manufacturing Personalized Medicine (CAMP), Singapore-MIT Alliance for Research and Technology Centre, Singapore, Singapore. [2]A*STAR Skin Research Labs (A*SRL), Singapore, Singapore. [3]Department of Biomedical Engineering, National University of Singapore, Singapore, Singapore. [4]Singapore Centre for Environmental Life Sciences Engineering, Life Sciences Institute, National University of Singapore, Singapore, Singapore. [5]Center for Biomedical Innovation, Massachusetts Institute of Technology, Cambridge, MA, USA. [6]Department of Electrical Engineering and Computer Science, Massachusetts Institute of Technology, Cambridge, MA, USA. ✉email: rajeev@mit.edu

Additionally, the pre-processing steps and subcultures part of the USP < 71 > workflow tend to be laborious, increase susceptibility to error, the risk of contamination and cost of goods[7]. These limitations are driving the use of alternative Rapid Microbiological Methods (RMMs). Commonly used RMMs includes the BACTEC™ (Becton Dickinson) and BACT/ALERT® 3D (bioMérieux), which are attractive over traditional methods for their shorter incubation period (7 days), automated continuous monitoring capability and objective detection of contamination[3]. Solid phase cytometry and flow cytometry are alternate RMMs that rely on staining of cells to identify labelled organisms. Other examples of RMMS include, nucleic acid amplification and isothermal microcalorimetry which involves a growth enrichment step over a period of time[8]. The short shelf lives of CTPs and the critical needs of patients demand approaches that are able to provide rapid detection of microbial contamination without compromising the final CTP[9].

Here, we present a machine-learning aided UV absorbance spectroscopy method as a potential approach for rapid, real-time microbial contamination detection. This novel assay couples an optical technique with a robust machine learning method that does not require large quantities of training data. With the recent push to utilize risk-based approaches to maintain the quality and safety CTPs[10], robust aseptic monitoring strategies are integrated in different CTP manufacturing stages to consistently assess the quality and safety status of the product[9]. The integration of process analytic technologies (PATs) such as UV absorbance spectroscopy with machine-learning elements could allow for automated, at-line monitoring of cell-culture for real-time contamination detection. Unlike current RMMs used in the CTP industry, the suggested approach is designed to be label-free, non-invasive (no cells required), requiring low sample volume and low-cost with no growth enrichment steps required.

For our studies, we have used mesenchymal stromal cell (MSC) cultures as a demonstrator as MSC therapies are widely used to treat acute tissue injuries, inflammatory diseases and chronic degenerative disorders[11]. The absorbance spectra of only sterile MSC culture samples, measured by a commercial spectrometer, is used to train a one-class support vector machine (SVM) model. An anomaly detection approach was deployed to identify spectral differences in the region of interest and predict contamination in test cell culture samples. We hypothesize that the spectral differences between nicotinic acid (NA) and nicotinamide (NAM) metabolites are underlying principles for the SVM model to predict contamination.

Our method was able to detect contamination at the 21-hour timepoint when 10 CFUs of *E. coli* was spiked in MSC culture from one donor (Donor A). Amongst the 7 commercial donors we had worked with, Donor A had performed better in correctly predicting sterile samples from other donors (Fig. S1). Thus, Donor A was preferentially selected as the donor to initially train the one-class SVM. In the following sections, we demonstrate the capability of the proposed method to detect down to 10 CFUs for 7 microorganisms and the robustness of this approach by testing across different commercial donor MSCs.

Results

Time to detection of *E. coli* using machine-learning aided UV absorbance spectroscopy

To demonstrate the sensitivity of the proposed method, the time to detection (TTD) of contaminants was investigated. Initial experiments used *E. coli K-12* (ATCC 25404) to establish sensitivity as it readily grows in nutrient-rich cell culture media such as Dulbecco's Modified Eagle Medium (DMEM). It is worth noting that cell therapy products derived from umbilical cord blood samples do find rare instances of E. coli contamination[9,12]. In the following sections, we expand this study to a larger set of microbes. Here, 10 CFUs of *E.coli* was inoculated into a single donor's (Donor A) MSC culture at 0-hour, and triplicate samples of supernatant were extracted at 3 hour intervals between 9 and 24 hour timepoints. Each collected sample inclusive of positive and negative controls was measured in triplicates with a spectrometer and its absorbance measurements (Fig. S2) were evaluated for contamination using an one-class SVM, that was trained on Donor A Phosphate Buffer Solution (PBS) spiked *sterile* samples.

Contamination was detected by the SVM model in the 10 CFUs of *E. coli* spiked samples after TTD ~ 21-hour. At this timepoint, the model predicted all negative control samples to be sterile and all positive control samples to be contaminated (100% true positive and true negative). The total time to detection was approximated to be 21.5 hours, inclusive of sample extraction, UV absorbance measurements and SVM analysis. We were able to conclude that the suggested method is able to detect contamination at low inoculums of *E. coli* (10 CFUs).

At each time point, the mean absorbance spectra of the negative control samples (Donor A MSC culture supernatant spiked with PBS) were subtracted from the mean spectra of positive control samples (fresh DMEM spiked with 1000 CFUs of *E. coli*) and mean spectra of test samples (10 CFUs of *E. coli* spiked samples). The resultant spectra were plotted as shown in Fig. 1. Over the course of time, the absorbance increase of the positive control samples is more significant (Fig. 1a) than the 10 CFUs of *E. coli* spiked samples (Fig. 1b). This could be attributed to the higher inoculum of *E. coli* (1000 CFUs) in the positive controls. A rapid increase in absorbance from 9-hour to 18-hour can be observed for the positive control samples, after which the absorbance gradually increases till the 24-hour timepoint. Changes in the absorbance spectra of the 10 CFUs of *E. coli* spiked samples were more apparent after the 18th hour (Fig. 1b) resulting in them predicted to be contaminated from the 21-hour timepoint.

The proposed method of machine-learning aided UV absorbance spectroscopy was compared with the gold standard compendial USP < 71 > test, BACT/ALERT® 3D[13] and a recently proposed sterility test based on the ratio of NA to NAM calculated via Liquid Chromatography-Mass Spectrometry (LC-MS)[14]. For UV absorbance spectroscopy and NA/NAM ratio using LC-MS analysis, cell cultures at 0-hour were inoculated with 10 CFUs of *E. coli* and collected every 3 hours for direct measurement starting from the 9th hour. To compare with the USP < 71>, aliquots of 1 mL of MSC culture containing 18 CFUs of *E. coli* was collected at 0-hour. Meanwhile, 10 CFUs of *E. coli* was prepared via serial dilution in Tryptic Soy Broth at 0-hour for BACT/ALERT® 3D[13]. A sample

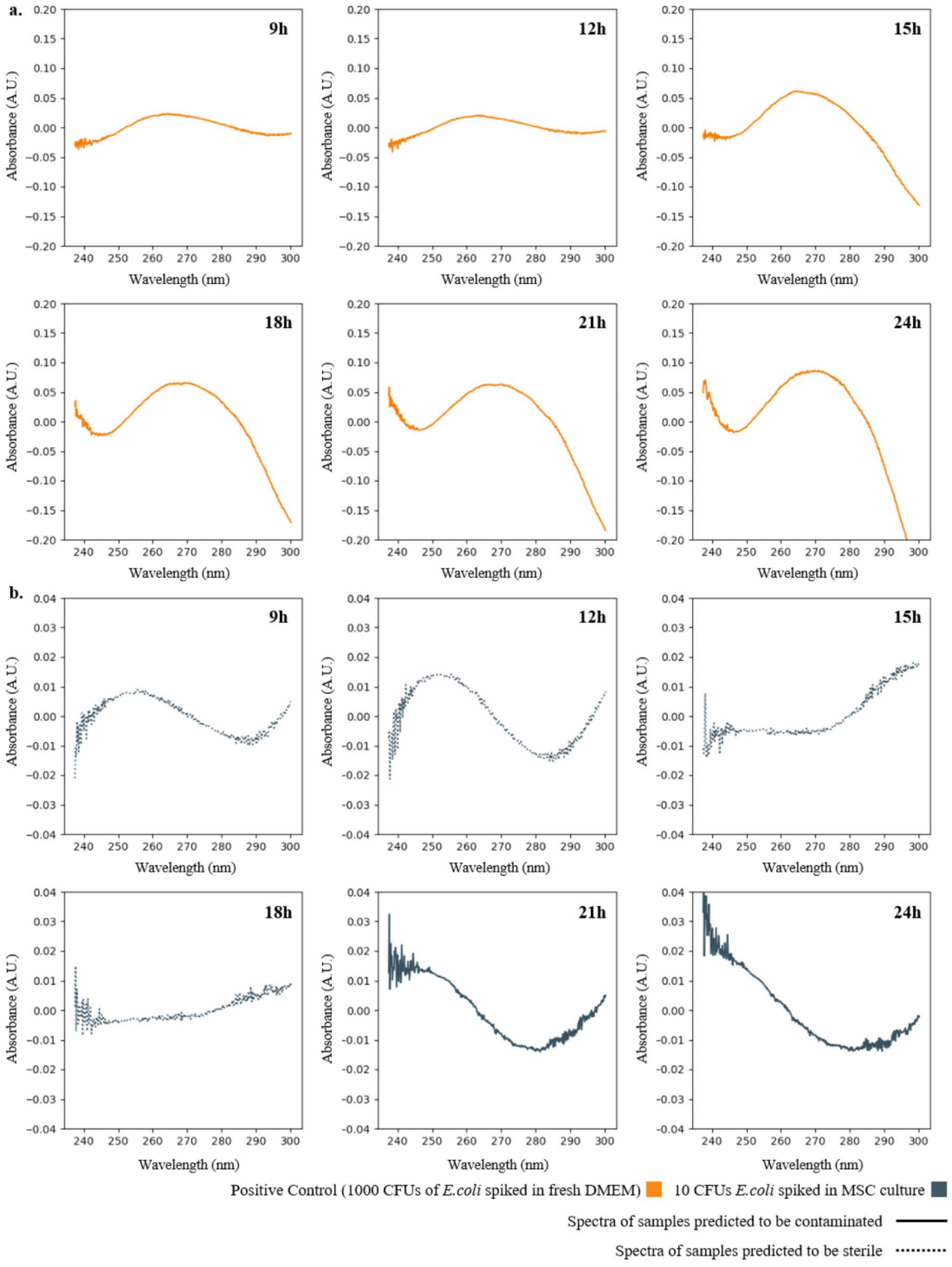

Fig. 1. Resultant mean absorbance spectra of *E. coli* spiked samples at 3 hour intervals between 9-hour and 24-hour timepoints. **a**. Resultant mean absorbance spectra of positive control *E. coli* spiked samples (orange) after subtraction of mean absorbance spectra of negative control samples of the same timepoint. Rapid increase in absorbance can be observed from 9-hour to 18-hour after which the rate of increase of absorbance becomes gradual. **b**. 10 CFUs (dark blue) *E. coli* spiked samples after subtraction of mean absorbance spectra of negative control samples of the same timepoint. Increase in absorbance is more significant for 21-hour and 24-hour timepoints.

of the contaminated cultures were inoculated into the respective aerobic and anaerobic mediums for compendial USP < 71 > test and BACT/ALERT® 3D.

Results showed that machine-learning aided UV absorbance spectroscopy has a comparable TTD of 21 h, to the USP < 71 > test (24 hours to observe turbidity) and the method of calculating ratio of NA to NAM via LC-MS (18 hours). However, the suggested approach took longer to detect contamination compared to BACT/ALERT® 3D (16 hours) suggesting that the sensitivity of our method might be lower.

The BacT/Alert® 3D requires additional inoculation of cell culture samples into multiple growth mediums (iNST and iAST), to test for the presence of aerobes and anaerobes at different incubation temperatures (30.5 –34.5 °C and 20.5 –24.5 °C respectively)[13]. Similarly, the compendial USP < 71 > test also requires samples to be inoculated in Soybean Casein Digest Medium and Fluid Thioglycollate Medium and incubated at 20 –25 °C and 30 –35 °C respectively[4]. Both BacT/Alert® 3D and USP < 71 > require the use of trained operators perform sample extraction from cell culture and inoculation into the various growth enrichment media used. These open processes are susceptible to operator variability and error, potentially compromising sterility and increasing risk of contamination[15]. The method of using the ratio of NA/NAM requires an additional centrifugation step after obtaining the supernatant, prior to LC-MS measurements. Whereas the suggested approach allows for direct absorbance measurements of the supernatant, allowing for the time taken for sample preparation to be minimized.

The UV absorbance spectroscopy method has a relatively simpler workflow as it does not require extra inoculation into growth enrichment media, additional incubation time and extra sample preparation. Instead, cell cultures can be directly collected for optical measurement with the UV-Vis spectrometer and analysis using the SVM model, therefore eliminating additional resources and cost associated with the growth enrichment inoculation step observed in BACT/ALERT® 3D and USP < 71>.

Detection of other microbial contaminants

To determine if the suggested method can be applied to other microbial organisms, a series of blinded validation studies were performed involving selected USP < 71 > organisms; *S. aureus* ATCC 6538, *P. paraeruginosa* ATCC 9027, *B. spizizenii* ATCC 6633, *C. sporogenes* ATCC 19404, yeast such as *C. albicans* ATCC 10231 and other microbial species; *E. coli K-12* (ATCC 25404) and slow-growing organisms including *C. acnes ATCC 6919*.

PBS spiked sterile Donor A samples, collected from days 2–7 of culture at passages 2,4 and 6, were used to train the SVM model. From the several Donor A MSC spent medium samples collected from passage 2–6, aliquots were randomly selected to prepare 10 CFUs and 100 CFUs microbe-spiked samples from the above-mentioned 7 organisms while some were used to prepare PBS spiked sterile samples (Table S1). The UV absorbance of these samples was measured and analysed with the SVM model, which was trained using Donor A PBS spiked sterile samples. The confusion matrix (Fig. 2) summarizes the prediction accuracies for the 80 measured samples. By training on sterile samples from Donor A and testing on samples from the same donor, the model was able to provide 100% true positive (detecting contaminated samples correctly) and 100% true negative (detecting sterile samples correctly) accuracies and was sensitive to a limit-of-detection (LoD) of 10 CFUs in detecting contamination caused by both fast and slow-growing organisms. Despite training on samples specifically from passages 2,4 and 6, the model was able to correctly predict the contamination status of samples from intermediary passages 3 and 5 (Table S1), giving confidence that the model does not pick up on media fluctuations between passages to predict contamination status.

To understand the underlying mechanism of the suggested approach, LC-MS studies on Donor A MSCs infected with different microbial species was analysed (Fig. 3) and the NA concentration was quantified. *P. paraeruginosa* infected Donor A MSC samples at 10 CFUs presented with NA levels 41 times higher than Donor A MSCs infected with *C. albicans* and *B. spizizenii*. In the case of *C. sporogenes*, no viable bacteria was detected in the LC-MS. We hypothesize that this could be due to the anaerobic nature of *C. sporogenes*, making it difficult to grow under normal MSC culture conditions. It is also possible for the bacteria to be killed as a result of possible

n = 80		Actual	
		Contaminated	Sterile
Predicted	Contaminated	75 [100%] *True Positive*	0 [0%] *False Positive*
	Sterile	0 [0%] *False Negative*	5 [100%] *True Negative*

Classification report	
Accuracy	100%
Precision	100%
Sensitivity	100%
Specificity	100%

Fig. 2. Confusion matrix and classification report for performance of one-class SVM model (trained on PBS spiked sterile Donor A samples) in correctly assessing sterility status of 80 Donor A test samples. 100% true positive rate (detecting contaminated samples correctly) and 100% true negative rate (detecting sterile samples correctly) were achieved.

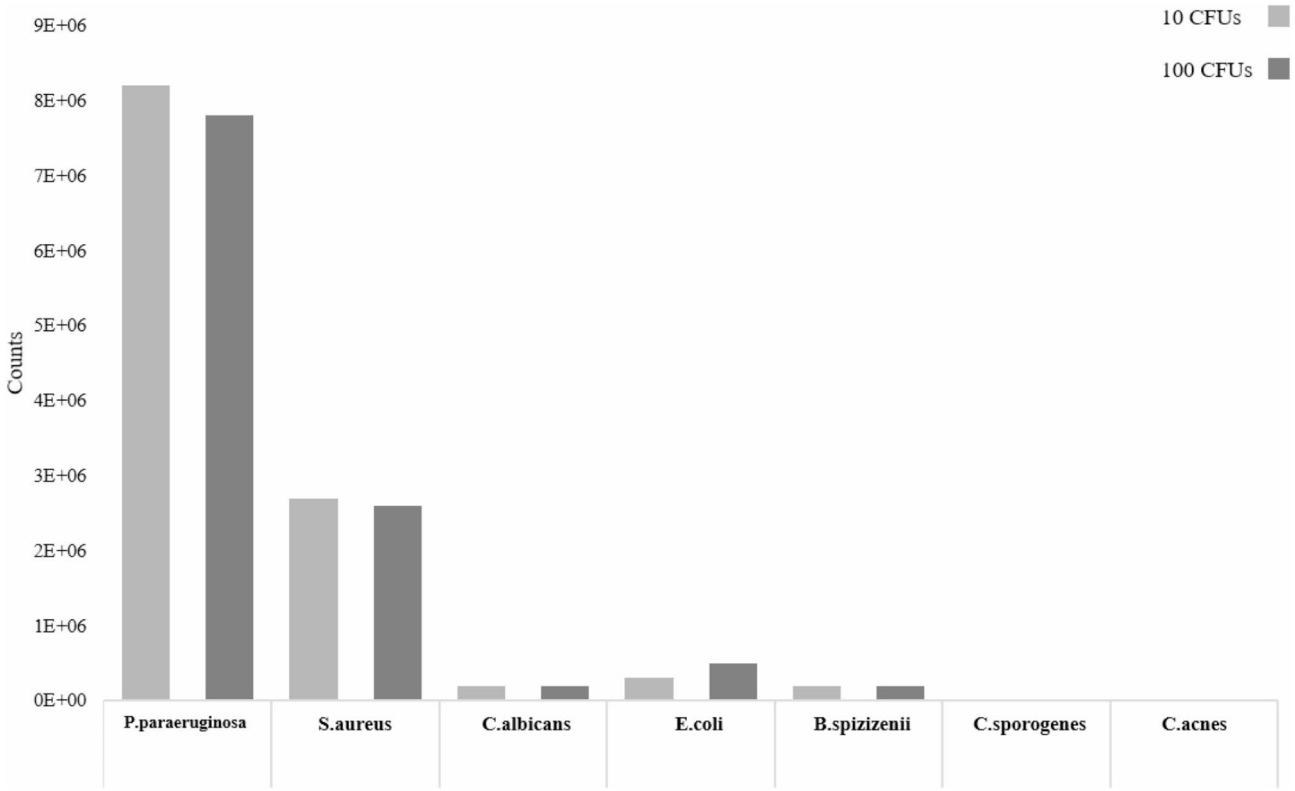

Fig. 3. LC-MS measurements illustrating concentration of NA in Donor A MSC culture samples inoculated with different microbial species at 10 and 100 CFUs in a 24 h incubation period. *P. paraeruginosa* spiked samples have the highest NA concentration, approximately 41 times higher than *C. albicans* and *B. spizizenii* infected samples at 10 CFUs. No NA was detected in *C. sporogenes* spiked samples due to possible antimicrobial activity of MSCs and no NA was detected in *C.acnes* spiked samples due to its slow-growing nature.

antimicrobial activity of MSCs[16]. The LC-MS studies were done within a 24-hour incubation period which was insufficient for slow-growing *C. acnes* to accumulate NA while *C. acnes* infected samples prepared for validation of machine-learning aided UV absorbance spectroscopy method had a culture time of 7 days prior to spiking into spent medium.

With *P. paraeruginosa* spiked samples having the highest concentration of NA on the LC-MS, Principal Component Analysis (PCA) was used to visualize the distribution of the training dataset samples and *P. paraeruginosa* spiked Donor A samples and thus gain insight into the performance of the SVM model. [Note that classification using PCA (linear) instead of SVM resulted in a significantly poorer assay performance, however PCA was useful for dataset visualization]. The PCA plot (Fig. S3a) shows that the *P. paraeruginosa* spiked samples were spread out and positioned further away from the PBS spiked sterile samples in the training dataset, clearly distinguishing between sterile and contaminated samples. The loading vectors of Principal Component 1 (PC 1) and Principal Component 2 (PC 2) were analysed as they account for the highest and second highest variances in the dataset. PC 1 and PC 2 loading vectors were plotted alongside the UV absorption spectra of 100 ug/ml NA and NAM spiked in PBS (Fig. S3b). The spectra were normalized at the 270 nm peak for better visualization. The PC 1 loading seems to have captured the maximum difference between NA and NAM at ~ 268 nm while PC 2 loading resembled one of the peaks of NA and NAM at ~ 270 nm.

Investigating robustness of machine-learning aided UV absorbance spectroscopy

Donor-to-donor variation is a critical bottleneck in the utility of MSCs which can potentially affect its therapeutic efficacy. This variation can be attributed to differences in tissue source, age, gender and physiological status[17]. As the donor's age increases, MSCs immunomodulation capabilities, proliferative abilities and differentiation potential decreases[18]. Thus, we wanted to further test the applicability of the developed model on test samples from other donors. To select robust donors for model training, we collected spent medium samples from 6 commercial donors (Donors B-G) from days 2–7 of cell culture at passage 2, 4 and 6 and prepared PBS spiked sterile samples from them. All the samples were then measured using the UV Vis spectrometer. The UV absorbance spectra of the PBS spiked sterile samples from one donor was used to train the SVM model and its accuracy in correctly predicting the PBS spiked sterile samples from other donors was then evaluated. Donors A and B had higher average prediction rates (81.2% and 65.6% respectively) in correctly predicting the PBS spiked

n = 418		Actual	
		Contaminated	Sterile
Predicted	Contaminated	329 [92.7%] *True Positive*	14 [22.2%] *False Positive*
	Sterile	26 [7.3%] *False Negative*	49 [77.7%] *True Negative*

Classification report	
Accuracy	90.4%
Precision	95.9%
Sensitivity	92.7%
Specificity	77.7%

Fig. 4. Confusion matrix and classification report summarizing SVM model (trained on PBS spiked Donor A and B samples) performance in assessing the sterility status of 418 test samples from 6 commercial MSC donors (donors B-G). Model achieved a 92.7% true positive accuracy and 77.7% true negative accuracy.

Microbial species	Limit-of-detection	Accuracy Correct prediction/Total samples
P. aeruginosa	10 CFUs/mL	30/30
S. aureus		28/28
C. albicans		26/26
B. subtilis		18/24
E. coli		18/23
C. sporogenes		24/25
C. acnes		30/33

Table 1. Limit-of-detection and accuracy of developed SVM model trained on Donors A and B for different microbial organisms at 10 CFUs.

sterile samples from the other donors (Fig. S1). Thus, the SVM model trained on donors A and B was deployed to predict samples from 6 other donors.

The donor A/B model was applied to an unseen test dataset (Table S2)– consisting of sterile and microbes spiked samples from 6 commercial donors. A total of 418 samples were analysed with the model and the confusion matrix (Fig. 4) summarizes the prediction accuracies of the retrained SVM model. A 92.7% true positive rate was achieved, with a consistent LoD of 10 CFUs for the 7 microbial organisms the model was tested with. At 10 CFUs, the lowest accuracy was for *B. spizizenii* samples (Table 1).

A true negative rate of 77.7% was attained. Analysing the 14 false positive samples, 10 samples were from Donor F. Fig. S1 suggests that Donors A and B have relatively low prediction accuracies for the Donor F 'sterile' samples. Further LC-MS analysis on selected Donor A and Donor B sterile samples (data not shown) revealed that the basal NA concentration for the samples that the model was trained with, approximated to be 1.6×10^4 counts. LC-MS analysis of Donor F 'sterile' samples had a NA concentration that exceeded 2×10^4 counts. The differences in NA concentration between Donor F and the training donors, may explain why the model predicts these Donor F samples to be outliers.

Discussion

Our proposed mechanism leverages preliminary studies that revealed a metabolite, NA – produced from the conversion of NAM via nicotinamidases, that could be an indicator of bacterial contamination[7]. The majority of documented nicotinamidases (88%) are found in bacterial genomes, thereby giving rise to NA production in most bacterial organisms[19]. Mammals, however, convert NAM directly into NAM mononucleotide and eventually NAD^+[20]. Thus, the presence of NA can be attributed to cell cultures contaminated with bacteria.

Several analytical techniques have been used to detect NA, ranging from colorimetric detection[21,22], thin layer chromatography[23–25] to spectrometric methods such as Raman spectroscopy[26] and UV absorbance spectroscopy[27,28]. Amongst these techniques, LC-MS[29–31] has been widely used as it has the potential to offer quantitative analyses with high selectivity and sensitivity[32].

With NA is being an essential vitamin, it can be consumed as a supplement to reduce low-density lipoprotein cholesterol and treat gastrointestinal diseases. Thus, there have been prior studies deploying UV absorbance spectroscopy to determine NA content in pharmaceutical dosage formulations. NA was dissolved in chemical solvents such as methanol and ethanol and measuring its absorbance using UV absorbance spectroscopy to construct a calibration curve[27,28].

To establish the baseline sensitivity of UV absorbance to detect NA and NAM, varying concentrations of NA and NAM dissolved in either PBS alone or a mixture of DMEM and PBS were prepared and measured using UV Vis spectrometer. In NA and NAM spiked PBS samples, both NA and NAM exhibit strong UV absorbance (Fig. 5a) in the 255–272 nm range - NA absorbance is stronger and three resonant absorption peaks are clearly observed. These distinct spectral differences will give rise to small changes in the UV absorbance spectra in contaminated cell culture media. These strong peaks could no longer be observed, when NA and NAM were spiked in DMEM and PBS (Fig. 5b(i)). The need to robustly detect these small spectral changes in complex medium formulations, such as DMEM, motivated the choice of a machine learning approach. With DMEM and PBS significantly contributing to the background noise, we selected the 6.25 ug/ml NA dissolved in DMEM and PBS to be subtracted from the 12.5 ug/ml – 100 ug/ml NA dissolved in DMEM and PBS samples. The same procedure was carried out for the NAM dissolved in DMEM and PBS samples and the resultant absorbance spectra were plotted. Figure 5b illustrates that the special features of NA and NAM could still be visualized after the background subtraction, giving confidence that the application of a machine learning approach would still be able to pick out these feature differences despite the strong background signals from DMEM and PBS. The ability to successfully detect low concentrations of NA and NAM in DMEM media, rich in amino acids, vitamins and metabolites, suggested the feasibility of using UV absorbance for contamination detection in cell culture media.

To further support the hypothesis that the NA, NAM spectral differences between NA and NAM are fundamentals for the SVM to detect contamination, we compared the model prediction against LC-MS analysis. This allowed us to establish that the changes in the UV absorbance could be correlated to the changes in NA and NAM metabolites detected by LC-MS quantitatively. LC-MS analysis of the samples obtained during the TTD experiment showed an increase in the NA to NAM ratio after the 18-hour timepoint for the 10 CFUs of *E. coli* spiked samples (Table 2). The SVM model was able to predict the 10 CFUs of *E. coli* spiked samples as contaminated after 21-hour. Samples where *only NA* was present such as the positive control samples at the 21 and 24 h time point (Fig.S4a), were predicted to be contaminated by the model. All negative control samples (Fig. S4b) together with positive control samples (Fig. S4a) at 9,12,15-hour timepoints and *E. coli* spiked samples from 9,12,15-hour timepoints (Fig.S4c,d) have *both NAM and NA*, yet the model correctly classifies the samples as sterile. Further analysis showed that 21 and 24-hour 10 CFUs of *E. coli* (Fig. S4c,d) samples with NA > 1.7×10^4 counts were predicted to be contaminated whereas samples that were predicted to be sterile had lower than 1.7×10^4 counts of NA.

The method described herein appears to detect contamination when the contaminant organisms express nicotinamidases. We have applied this method to 7 microorganisms, inclusive of selected USP < 71 > isolates, which were detected at low concentrations of 10 CFUs. This LoD is equivalent to that of the USP < 71 > and BACT/ALERT® 3D. Previous studies have performed a tBLASTn which highlighted that *C. sporogenes* lacked the *pncA* gene encoding for nicotinamidases, implying that nicotinic acid would not be produced[14]. The same analysis reported that that the conspecific *C. sporogenes* ATCC 15579 genome contains a nicotinamidase-encoding gene, thus concluding that the tBLASTn might not be fully accurate or that the genome incompleteness implies a false negative. The presence of a non-canonical nicotinamidase may be another possibility. Our studies involved testing the SVM model with *C. sporogenes* ATCC 19404 spiked samples, which were predicted to be contaminated. In addition, testing *C. sporogenes* ATCC 19404 spiked samples at 5 and 10 CFUs using LCMS revealed a high concentration of NAM and a relatively low concentration of NA (Fig. 6). Since NA can also be observed in the *C. sporogenes* ATCC 19404 via LCMS and machine-learning aided UV absorbance spectroscopy, further analysis should be performed on different *C.sporogenes* strains to examine the presence of *pNCA* gene.

Training on 2 commercial donors with good prediction accuracies across other donors and testing on all donors revealed that the donor-to-donor variability observed between MSC donors affects the true negative rate of the model. Analysing the false positives, approximately 71.4% of the samples belonged to Donor F, which were not well predicted by a classifier trained on sterile samples from Donors A and B possibly due to the 25% higher level of NA even in the 'sterile' Donor F samples. After exclusion of Donor F sterile and contaminated samples, the model had a higher true negative rate of 92% and lower false positive rate of 8% while maintaining the true positive accuracy ~ 91% across five donors (Donors B-E and G).

Conclusion

We have presented data supporting initial proof-of-principal demonstration of a rapid sterility test that is simple, economic, non-invasive (cell-free) and label-free for microbial contamination detection. Our technique incorporates UV absorbance spectroscopy and a one-class SVM model that is purely trained on absorbance spectra of sterile supernatant samples of MSCs. We have performed TTD experiments to show that 10 CFUs of *E. coli* can be detected clearly after the 21-hour timepoint. Moreover, the use of our method has been demonstrated to detect 10 CFUs of selected USP < 71 > isolates including yeast (*C. albicans*), contaminants like *E.coli* and slow-growing *C. acnes*, with an average true positive rate of 92%. Aspects of donor-to-donor variability has been explored by training the SVM model on 2 donors and to testing on 6 donors. This detection technique involves minimal sample preparation, without any need for specific growth media, additional sub-culturing or incubation period. Previous work has established that NA metabolite produced from the conversion of NAM by microbial nicotinamidases serves as an indication of contamination in mammalian cell cultures. With NA and NAM having significant spectral features in the UV region, we hypothesize that the spectral differences between NA and NAM enable the differentiation between sterile and contaminated samples.

Despite its advantages, there are several limitations to the initial study presented here. Further validation experiments must be performed with a variety of microbial contaminants representative of the flora of cGMP environments and indicative of prior contamination CTPs. This would also include determining the applicability of the proposed approach to detect contamination caused by yeasts and fungi. Secondly, since NA is present in a

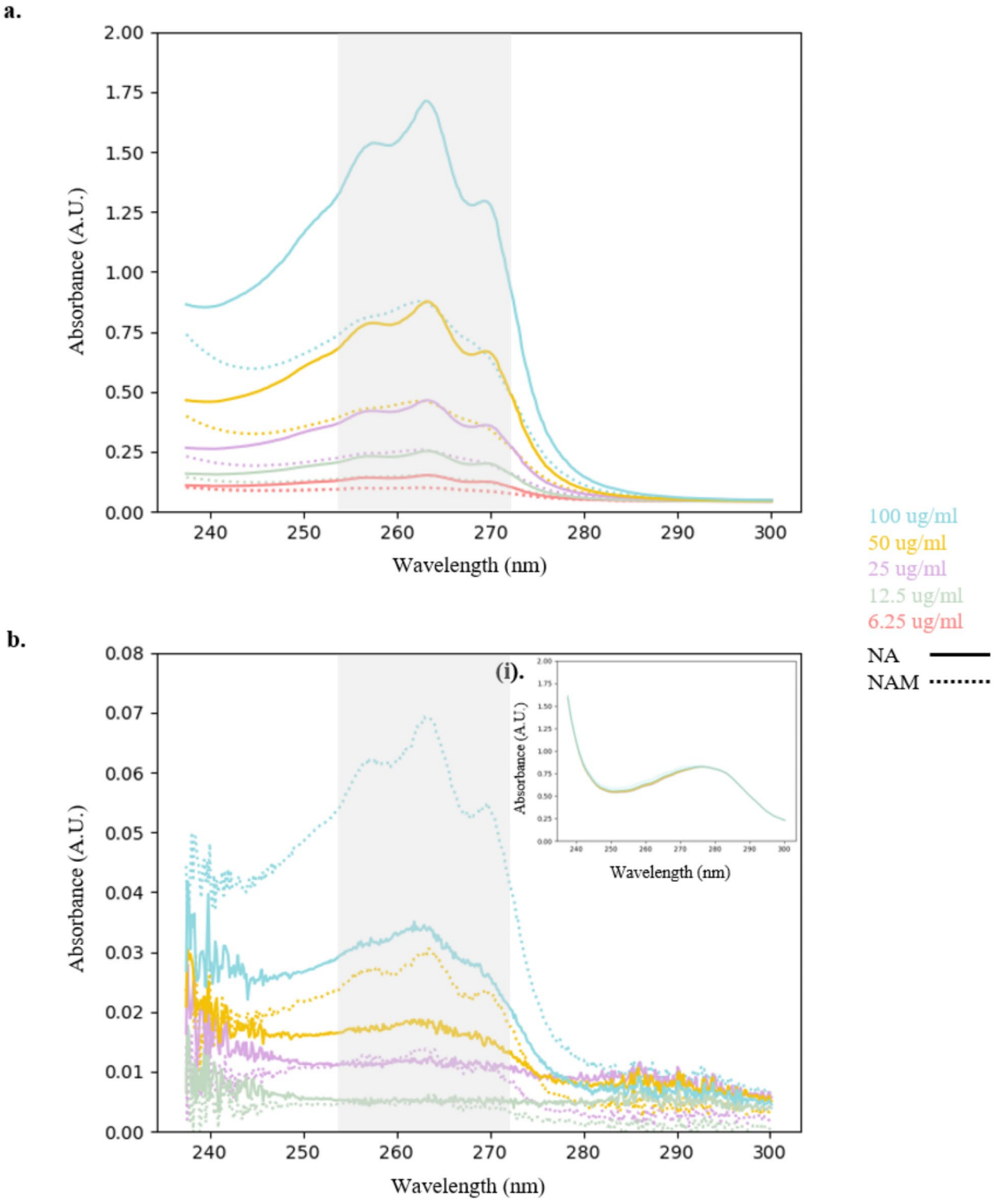

Fig. 5. Absorbance spectra of NA and NAM measured using UV-Vis spectrometer. **a**. Absorbance spectra of varying concentrations (6.25 ug/ml – 100 ug/ml) of NA and NAM dissolved in PBS respectively. NA spiked samples have stronger absorbance than NAM spiked samples. Three resonant peaks are clearly observed within region of interest (255–272 nm) **b.** Resultant NAM spectra (dashed lines) after spectrum of 6.25 ug/ml NAM spiked in DMEM and PBS were subtracted from higher concentrations of NAM spiked in DMEM and PBS. Resultant NA spectra (solid lines) after spectrum of 6.25 ug/ml NA spiked in DMEM and PBS were subtracted from higher concentrations of NA spiked in DMEM and PBS spectra. Peaks of NA and NAM could be seen after background subtraction. (i) Spectra of varying concentrations of NA and NAM (6.25 ug/ml–100 ug/ml) spiked in DMEM and PBS, where peaks of NA and NAM can no longer be observed.

Timepoint	Sample type	LC-MS	SVM
9h	10 CFUs/mL E.coli spiked		
	18 CFUs/mL E.coli spiked		
	Negative control		
	Positive control		
12h	10 CFUs/mL E.coli spiked		
	18 CFUs/mL E.coli spiked		
	Negative control		
	Positive control		
15h	10 CFUs/mL E.coli spiked		
	18 CFUs/mL E.coli spiked		
	Negative control		
	Positive control		
18h	10 CFUs/mL E.coli spiked		
	18 CFUs/mL E.coli spiked		
	Negative control		
	Positive control		
21h	10 CFUs/mL E.coli spiked		
	18 CFUs/mL E.coli spiked		
	Negative control		
	Positive control		
24h	10 CFUs/mL E.coli spiked		
	18 CFUs/mL E.coli spiked		
	Negative control		
	Positive control		

Predicted contaminated
Predicted sterile

Table 2. Comparison of LC-MS results and SVM model prediction for each timepoint in TTD experiment. At each time point, a negative control, positive control and 10 CFUs *E.coli* spiked sample were collected in triplicates. Each collected sample was measured in triplicates using LC-MS and UV absorbance spectroscopy. Measured spectra was analysed with developed SVM model. LC-MS analysis and SVM model have been consistent for all negative and positive control samples. LC-MS analysis was able to detect contamination at 18-hour timepoint for 10 CFUs *E.coli* spiked samples, SVM model was able to detect contamination at 21-hour timepoint.

wide range of microbial species and different organisms have different NA production rates, the TTD cannot be generalized using *E.coli* only. Further studies investigating the TTD of a broad range of microorganisms remain to be performed. Additionally, the model should be tested with more stem cell types. Aside from MSC studies, this technology can be tested with CAR T-cells[34], haematopoietic stem cells[35] and human induced pluripotent stem cells[1]. For each cell type, it is crucial to expand the range of training donors from different demographics.

Our goal was to develop a technique which requires a low sample volume (< 1 mL) and short turnaround time (< 30 minutes) for real-time microbial contamination detection but is sufficiently robust to provide results with high sensitivity and specificity. This approach was designed to be implemented as part of the CTP manufacturing process, as a form of preliminary testing that users can rely on for early signs of contamination. Should the approach described herein predict the sample to be contaminated (over a few hours), established RMMs such as BACT/ALERT® 3D system can be subsequently used to confirm the test results. While the anomaly detection algorithm demonstrated here does not identify the specific microbial contaminant, it is advantageous compared to culture-based methods due to its rapid outcome, non-invasiveness (no cells required) and simple workflow. The incorporation of rapid sterility test methods into CTP manufacturing as a form of continuous safety testing, allows for more timely implementation of corrective actions, should a contamination event occur.

In recent times, the use of automated technologies in the CTP manufacturing process is desired to minimize variability and reduce the dependence on labour for procedures such as sample extraction, preparation, analysis[36]. The proposed approach is amenable to be integrated with at-line sampling systems such as the MAST sampling system *(Milipore Sigma, Burlington, MA, USA)* allowing for periodic, aseptic sampling of cultures from upstream bioreactors to downstream PATs for analysis. Furthermore, automated UV absorbance spectroscopy systems can be interfaced; allowing for automated spectral measurements of extracted culture samples in an optical flow cell. Synchronizing automated sampling systems and PATs with our proposed method enables cell cultures to be monitored continuously, allowing for contamination to be caught at low inoculums during in-process monitoring.

Methods

Materials

Nicotinic acid (NA) and Nicotinamide (NAM) powder (Catalog No: 72309, 72340) were purchased from Sigma-Aldrich. Bacterial strains *P. paraeruginosa* (ATCC 9027), *S. aureus* (ATCC 6538), *C. albicans* (ATCC 10231), *B.*

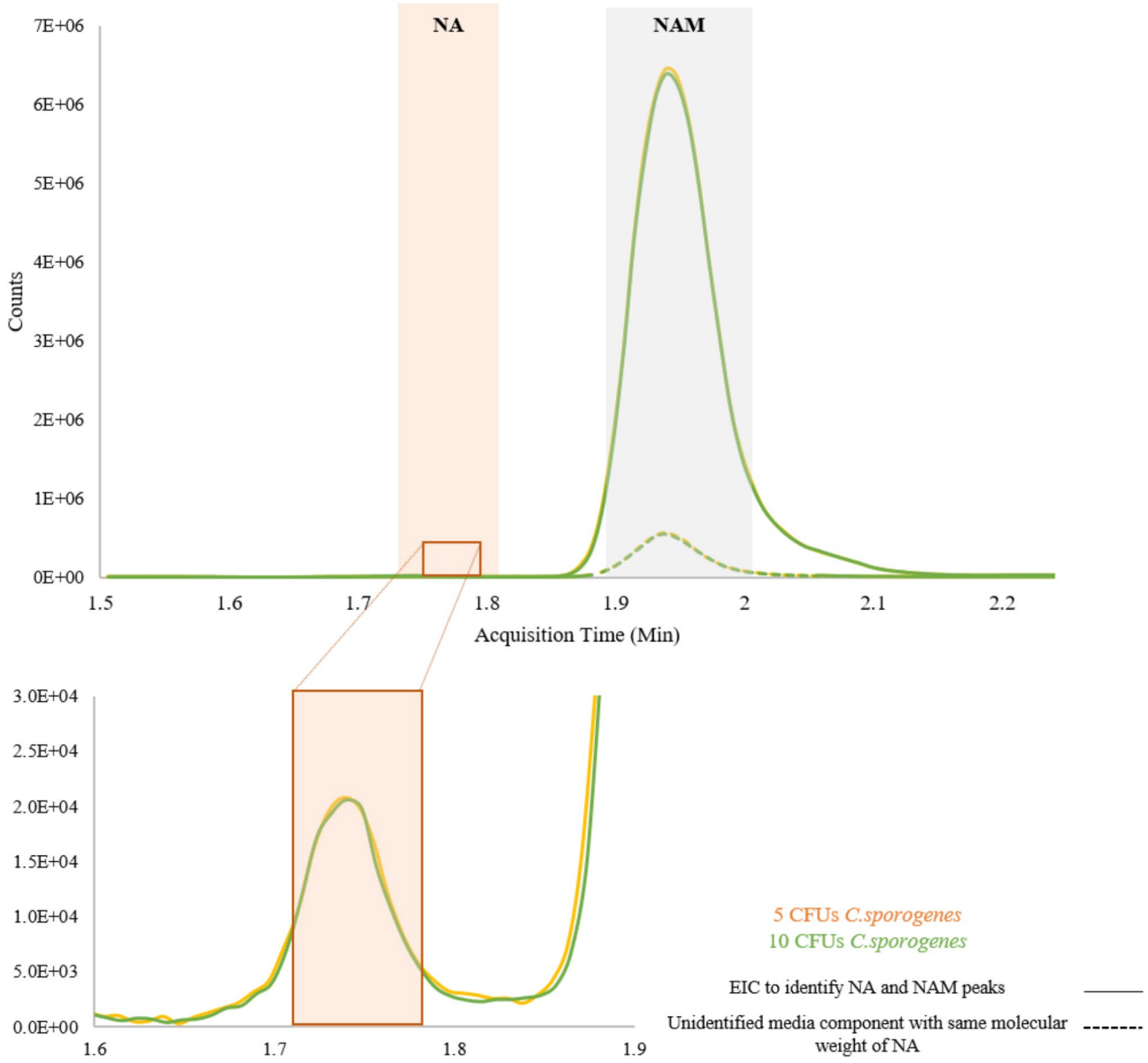

Fig. 6. LC-MS analysis for culture mediums spiked with 5 CFUs and 10 CFUs *C. sporogenes* spiked samples. Representative examples of Extracted Ion Chromatograms (EIC) of *C.sporogenes* contaminated MSC cultures with highlighted regions of NA and NAM. Identification of NAM peak at ~ 1.98 min and NA peak at ~ 1.74 min. A high concentration of NAM and low concentration of NA was observed in these samples.

spizizenii (ATCC 6633), *E. coli K-12* (ATCC 25404), *C. sporogenes* (ATCC 19404), *C. acnes* (ATCC 6919) were obtained from the American Type Culture Collection.

Preparation of varying concentrations of NA and NAM in PBS

0.2 mg of NA powder was dissolved in 1mL of PBS to prepare a 200 ug/mL stock solution. Subsequently, 5 concentrations (100 ug/mL, 50 ug/mL, 25 ug/mL, 12.5 ug/mL and 6.25 ug/mL) were prepared via serial dilutions, as 1 mL samples. 600 uL per sample was used for measurements with the UV-Vis spectrometer. The same procedure was repeated with NAM. These samples are referred to as *NA and NAM spiked in PBS samples* throughout the paper.

Human bone-marrow-derived MSCS isolation and culture

Bone-marrow-derived MSCs from seven adult human donors were obtained from a commercial source *(Lonza)* at passage 1. MSCs were cultured in a T-175 culture flask containing DMEM cell culture media supplemented with 10% fetal bovine serum (FBS) without the addition of antibiotics. The cells were incubated at 37℃ with 5% CO_2 and fresh media was replenished twice a week. The cells were passaged at a confluency of 70%. Spent

	Organism	Nutrient broth used	Culture time	Incubation temperature	Respiration
USP < 71 > isolates	*P. paraeruginosa* (ATCC 9027)	LB	O/N	37℃	Aerobic
	S. aureus (ATCC 6538)	LB	O/N	37℃	Aerobic
	B. spizizenii (ATCC 6633)	LB	O/N	33℃	Aerobic
	C. albicans (ATCC 10231)	YPD	O/N	33℃	Aerobic
	C. sporogenes (ATCC 19404)	RCM	2 days	37℃	Anaerobic
Other isolates	*E. coli* K-12 (ATCC 25404)	LB	O/N	37℃	Aerobic
	C. acnes (ATCC 6919)	BHIB	7 days	33℃	Anaerobic

Table 3. Summary of microbial organisms and its respective culture conditions used over the course of this study. LB: Luria – Bertani broth; YPD: Yeast Peptone Dextrose; RCM: Reinforced Clostridial Medium broth, BHIB: Brain Heart Infusion broth. O/N: overnight.

medium from the donors collected from day 2 to 7, at passages 2 to 6 were frozen in 15 mL falcon tubes and subsequently thawed for further experiments.

Preparation of PBS spiked sterile samples

Frozen spent medium samples were thawed in a dry bath. 2.4mL of spent medium was aliquoted into fresh 15 mL falcon tubes, from which 100 uL of spent medium was removed and replaced with 100 uL of PBS. These samples have been referred to as *PBS spiked sterile samples* over the course of the paper.

Preparation of microbes inoculated samples

One colony of each organism was picked, cultured and incubated in a 15 mL falcon tube containing 5 mL of the respective nutrient broth. Table 3 summarizes the different broths, culture times and incubation temperatures used for different microbial organisms. An anaerobic container was used to culture *C. sporogenes* (ATCC 19404) and *C. acnes* (ATCC 6919).

Post culture of the microbial organisms, the optical density (OD) of 1 mL of microbial solution is measured with the OD reader and diluted to OD 0.075 (in 5 mL of the respective broth) and incubated for further subculture to reach log-phase. The sub-cultured microbial cells were harvested by centrifugation at 7000xg, for 10 min. Subsequently, the microbial cells were concentrated in 2 mL PBS. The microbial solution was then diluted 10-fold, with 1 mL of microbial solution diluted with 9 mL PBS (achieving OD 0.1). Serial dilutions of the bacteria were carried out as follows:

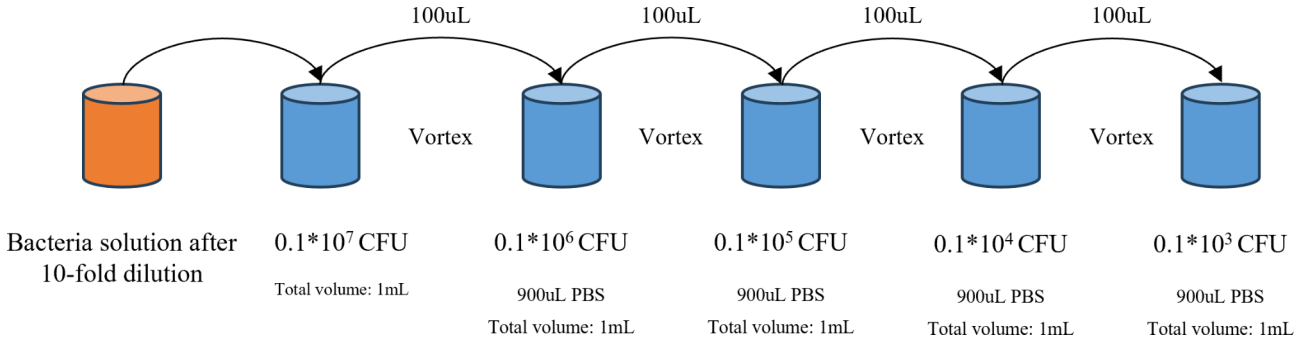

To spike 100 CFU of microbial species, aliquot 100uL from [$0.1*10^4$ CFU] tube into 2.3 mL of thawed MSC spent media in a 15 mL tube. Lastly, to spike 10 CFU of microbial species, aliquot 100uL from [$0.1*10^3$ CFU] tube into 2.3 mL of thawed MSC spent media in a 15 mL tube. Samples are measured immediately after spiking. Additionally, a sample from the respective tube is plated and incubated overnight. CFU plate counting is performed the next day to verify the inoculated CFU.

MSCs inoculated with *E. coli* for time detection experiments

MSCs were cultured according to the methods described above till passage 5 was attained. The cells were then trypsinized from the T-175 flask and seeded at 10^5 cells/well in 6 well plates and incubated overnight at 37℃ and 5% CO_2. 10 CFUs of *E.coli* and 1000 CFUs of *E.coli* were prepared as mentioned above. 1000 CFUs of *E. coli* spiked into blank DMEM media was used as positive control whilst untreated MSCs supernatant were used in the preparation of negative control. The negative control samples prepared with for UV absorbance measurements were additionally spiked with PBS following the above-mentioned methods.

10^5 cells/mL were inoculated with 10 CFUs *E. coli* and incubated for 24 h. Intermittently, samples were drawn at 3 h intervals from 9 h to 24 h. Collected samples were spun down to obtain supernatant only. All supernatant samples were split into pairs – for LC-MS and UV absorbance measurements respectively. The supernatant

samples for LC-MS measurements were filtered through a Nanosep centrifugal device with an Omega 10 K molecular weight cut-off membrane *(Pall Corporation, Port Washington, NY, USA).*

Selection of suitable PAT

Previous work using NA/NAM ratio as a marker for sterility utilized LC-MS. As LC-MS requires specialized trained personnel for operation of expensive instrument rapid PATs were considered. As discussed above, the literature reports several analytical techniques to detect NA, ranging from colorimetric detection[21,22], thin layer chromatography[23–25] to spectrometric methods such as Raman spectroscopy[26] and UV absorbance spectroscopy[27,28]. UV absorbance was chosen for this work because it is reagent-free and has better sensitivity than Raman spectroscopy. Furthermore, widely available, commercial UV spectrophotometers can be used to perform the proposed assay.

UV-absorbance spectrometer measurements

A standard UV quartz cuvette of 2 mm path length and 600 uL sample volume was used with a commercial UV-Vis spectrometer *(Cary 60, Agilent Technologies, Santa Clara, CA, USA)* to measure the absorbance of the samples. A scan rate of 180 nm/min and data interval of 0.15 nm were set as parameters in the UV-Vis spectrometer. Triplicates were measured for each sample from 225 nm to 600 nm. The cuvette was washed thoroughly with MiliQ water between samples to avoid cross-contamination between samples. The cuvette was then dried using a Kim wipe before being used with subsequent samples.

As the samples from blinded validation studies and test dataset from different donors were measured over a series of days, PBS aliquots were measured at the start and end of each day to ensure that the UV-Vis is well calibrated and is not experiencing heavy instrumentation drifts which can cause spectral shifts.

UV-absorbance spectral processing

A pre-processing step was implemented to adjust any spectral divergences. Raw spectra of samples measured using the UV-Vis spectrometer is mean-centred before being analysed by the model. This processing step appears to alleviate variations that would otherwise result in false classifications of contamination. The protocol corrects for different bacteria strains having different baseline changes in UV absorbance (Fig.S5a): *P. paraeruginosa*, *S. aureus* and *C. albicans* spiked samples have a higher absorbance, whereas the spectra of *E. coli*, *B. spizizenii*, *C. sporogenes*, *C. acnes* samples are relatively similar to the training dataset.

Other instances of spectral divergences include, cuvette containing water traces from washing of the cuvette after measurements, resulting in lower absorbance of subsequent sample (Fig.S5*b)*. Furthermore, as sample measurements are taken over a long period of time, instrumentation drift can occur. As spectral deviations will result in samples to be predicted as outliers by the model, we have found that analysis using a mean-centered UV spectrum removes false positives from all three sources.

Selection of suitable machine-learning algorithm

A Partial Least Squares (PLS) algorithm was initially used to predict the concentration. The PLS worked well in NA spiked in DMEM samples, with a limit of detection of 3.125 ug/mL. However, when used to predict the concentration of NA in cell culture samples, the PLS training was sensitive to fluctuations in other media components, resulting in inaccurate NA estimates and predictions of contamination. Several other anomaly detection algorithms such as Isolation Forest, Local Outlier Factor were considered. Usage of these algorithms produced true positive accuracies (< 75%). The one-class SVM, used here, yielded the best results (> 90% true positive accuracy).

Construction of SVM model

A one-class SVM (imported from https://scikit-learn.org/stable/modules/generated/sklearn.svm.OneClassSVM.html) with a *rbf* kernel, a gamma value of 0.002 and nu value of 0.2 was applied in the development of the model. Every sample measured using the *Cary 60* was exported as a .csv file consisting of the absorbance values of its triplicates corresponding to each wavelength point. As the most prominent features of nicotinic acid and nicotinamide lies within 230 nm to 280 nm, only the absorbance values from 237 to 300 nm were used for model training and testing. This helps to avoid noise in other parts of the spectrum to be picked up as significant by the model. All samples are mean-centred to account for any spectral deviations caused by factors such as instrumentation drifts.

PBS spiked sterile samples from Donor 5 and Donor 8 at passages 2,4,6 from days 2 to 7 were used in the training of the model. These samples were labelled as 1 to denote the status of the samples as sterile. SVM model was then implemented to predict the contamination status of an unlabelled test dataset. An output label of -1 would indicate that the model predicts for a particular sample to be contaminated whilst an output label of 1 would indicate that the model predicts for that sample to be sterile.

LC-MS data analysis

Raw spectrometric data was analysed using MassHunter Workstation Qualitative Analysis software V10.0 (imported from https://www.agilent.com/en/product/software-informatics/mass-spectrometry-software/data-analysis/qualitative-analysis) and MassHunter Workstation Quantitative Analysis software V10.1 (imported from https://www.agilent.com/en/product/software-informatics/mass-spectrometry-software/data-analysis/quantitative-analysis) *(Agilent Technologies, Santa Clara, CA, USA)*. A Molecular Feature Extraction algorithm utilizing samples retention time and accurate mass was used to extract the molecular features of the peaks. MassHunter Workstation Mass Profiler Professional software V15.1 (imported from https://www.agilent.com/en/product/software-informatics/mass-spectrometry-software/data-analysis/mass-profiler-professional-software) was utilized

to visualize and analyse molecular features. Molecular weight of 122.06 at a retention time of 1.98 min was used to identify NAM peaks and a molecular weight of 123.04 at a retention time of 1.74 min was used to identify NA peaks. The MassHunter Quantitative Analysis software was used to calculate the area under the peaks at the specified retention times of NA and NAM.

Data availability

The datasets generated and analysed for the current study are available from the corresponding author upon reasonable request.

Received: 8 August 2024; Accepted: 11 December 2024
Published online: 04 March 2025

References

1. Hoang, D. M. et al. Stem cell-based therapy for human diseases. *Sig. Transduct. Target. Ther.* **7**, 1–41 (2022).
2. Ali, S. Microbial and viral contamination of animal and stem cell cultures: Common contaminants, detection and elimination. *JSRT* 2, (2017).
3. Gebo, J. E. T. & Lau, A. F. Sterility testing for cellular therapies: What is the role of the clinical microbiology laboratory? *J. Clin. Microbiol.* **58**, e01492–e01419 (2020).
4. USP. 71 STERILITY TESTS.pdf.
5. England, M. R., Stock, F., Gebo, J. E. T., Frank, K. M. & Lau, A. F. Comprehensive evaluation of compendial USP < 71>, BacT/alert dual-T, and Bactec FX for detection of product sterility testing contaminants. *J. Clin. Microbiol.* **57**, e01548–e01518 (2019).
6. Panch, S. R. et al. A prospective evaluation of a practical guideline for managing positive sterility test results in cell therapy products. *Biol. Blood Marrow Transpl.* **25**, 172–178 (2019).
7. Doulgkeroglou, M. N. et al. Automation, monitoring, and standardization of cell product manufacturing. *Front. Bioeng. Biotechnol.* **8**, (2020).
8. Bonnevay, T. et al. The development of compendial rapid sterility tests. *Pharmacopeial Forum*. **43**, (2017).
9. Cundell, T., Atkins, J. W. & Lau, A. F. Sterility testing for hematopoietic stem cells. *J. Clin. Microbiol.* **61**, e01654–e01622 (2023).
10. Iancu, E. M. & Kandalaft, L. E. Challenges and advantages of cell therapy manufacturing under Good Manufacturing Practices within the hospital setting. *Curr. Opin. Biotechnol.* **65**, 233–241 (2020).
11. Galipeau, J. & Sensébé, L. Mesenchymal stromal cells: Clinical challenges and therapeutic opportunities. *Cell. Stem Cell.* **22**, 824–833 (2018).
12. Ko, Y. K. et al. Reducing microbial contamination in hematopoietic stem cell products and quality improvement strategy: Retrospective analysis of 1996–2021 Data. *Ann. Lab. Med.* **43**, 477–484 (2023).
13. Günther, S. K., Geiss, C., Kaiser, S. J., Mutters, N. T. & Günther, F. Microbiological control of cellular products: The relevance of the cellular matrix, incubation temperature, and atmosphere for the detection performance of automated culture systems. *Transfus. Med. Hemother*. **47**, 254–263 (2020).
14. Huang, J. et al. The ratio of nicotinic acid to nicotinamide as a microbial biomarker for assessing cell therapy product sterility. *Mol. Ther. Methods Clin. Dev.* **25**, 410–424 (2022).
15. Spectroscopic methods and. their applicability for high-throughput characterization of mammalian cell cultures in automated cell culture systems. https://doi.org/10.1002/elsc.201500122
16. Alcayaga-Miranda, F., Cuenca, J. & Khoury, M. Antimicrobial activity of mesenchymal stem cells: Current status and new perspectives of antimicrobial peptide-based therapies. *Front. Immunol.* **8**, 339 (2017).
17. Goh, D., Yang, Y., Lee, E. H., Hui, J. H. P. & Yang, Z. Managing the heterogeneity of mesenchymal stem cells for cartilage regenerative therapy: A review. *Bioengineering* **10**, 355 (2023).
18. Zha, K. et al. Heterogeneity of mesenchymal stem cells in cartilage regeneration: From characterization to application. *npj Regen. Med.* **6**, 1–15 (2021).
19. Sánchez-Carrón, G. et al. Biochemical and mutational analysis of a novel Nicotinamidase from Oceanobacillus iheyensis HTE831. *PLoS One*. **8**, e56727 (2013).
20. Zapata-Pérez, R., García-Saura, A. G., Jebbar, M., Golyshin, P. N. & Sánchez-Ferrer, Á. Combined whole-cell high-throughput functional screening for identification of new nicotinamidases/pyrazinamidases in metagenomic/polygenomic libraries. *Front. Microbiol.* **7**, (2016).
21. Bandier, E. & Hald, J. A colorimetric reaction for the quantitative estimation of nicotinic acid. *Biochem. J.* **33**, 264–271 (1939).
22. Swaminathan, M. A Colorimetric method for the estimation of nicotinic acid in foodstuffs. *Nature* **141**, 830–830 (1938).
23. Frei, R. W., Kunz, A., Pataki, G., Prims, T. & Zürcher, H. The determination of nicotinic acid and nicotinamide by thin-layer chromatography and in situ fluorimetry. *Anal. Chim. Acta*. **49**, 527–534 (1970).
24. Navas Díaz, A., Guirado Paniagua, A. & García Sánchez, F. Thin-layer chromatography and fibre-optic fluorimetric quantitation of thiamine, riboflavin and niacin. *J. Chromatogr. A*. **655**, 39–43 (1993).
25. Vilter, S. P., Spies, T. D. & Mathews, A. P. A method for the determination of nicotinic acid, nicotinamide, and possibly other pyridine-like substances in human urine. *J. Biol. Chem.* **125**, 85–98 (1938).
26. Sala, O., Gonçalves, N. & Noda, L. Vibrational analysis of nicotinic acid species based on ab initio molecular orbital calculations. *J. Mol. Struct. –J. Mol. Struct.* **565**, 411–416 (2001).
27. Chanda, I., Bordoloi, R., Chakraborty, D. D., Chakraborty, P. & Das, S. R. C. Development and validation of UV-spectroscopic method for estimation of niacin in bulk and pharmaceutical dosage form. *J. App. Pharm. Sci.* **7**, 081–084 (2017).
28. Nwanisobi, G. & Ukoha, P. Spectrophotometric determination of niacin using 2,3-dichloro-5,6-dicyano-1,4-benzoquinone. *Asian J. Chem.* **28**, 2371–2374 (2016).
29. Roy, B., Singh, B., Rizal, A. & Malik, C. P. Bioanalytical method development and validation of niacin and nicotinuric acid in human plasma by. *LC–MS/MS* **6**, (2014).
30. Liu, M. et al. Simultaneous quantification of niacin and its three main metabolites in human plasma by LC–MS/MS. *J. Chromatogr. B*. **904**, 107–114 (2012).
31. Vats, P., Verma, S. M., Monif, T. & Novel LC–MS/MS method for estimation of niacin with negligible matrix effect and its application to the BE study. *J. Pharm. Invest.* **47**, 241–248 (2017).
32. Dettmer, K., Aronov, P. A. & Hammock, B. D. Mass spectrometry-based metabolomics. *Mass. Spectrom. Rev.* **26**, 51–78 (2007).
33. Parveen, S. et al. Evaluation of growth based rapid microbiological methods for sterility testing of vaccines and other biological products. *Vaccine* **29**, 8012–8023 (2011).
34. Alnefaie, A. et al. Chimeric antigen receptor T-cells: An overview of concepts, applications, limitations, and proposed solutions. *Front. Bioeng. Biotechnol.* **10**, 797440 (2022).
35. Bashor, C. J., Hilton, I. B., Bandukwala, H., Smith, D. M. & Veiseh, O. Engineering the next generation of cell-based therapeutics. *Nat. Rev. Drug Discov.*. **21**, 655–675 (2022).
36. Aifuwa, I. PAT strategies and applications for cell therapy processing. *Curr. Opin. Biomed. Eng.* **24**, 100405 (2022).

Acknowledgements
This work was supported by the National Research Foundation, Prime Minister's Office, Singapore under its Campus for Research, Excellence and Technological Enterprise (CREATE) program, through Singapore-MIT Alliance for Research and Technology (SMART): Critical Analytics for Manufacturing Personalized-Medicine (CAMP) Interdisciplinary Research Group.

Author contributions
S.P.C.: conceptualization, data curation, investigation, methodology, validation, formal analysis, writing-original draft preparation, writing-reviewing and editing A.N.J.Y.: data curation, investigation, methodology, formal analysis J.H.: conceptualization, investigation, methodology E.L.: conceptualization, investigation, methodology M.B.: conceptualization, investigation, methodology D.Y.: conceptualization, writing-reviewing, supervision R.B.H.W.: conceptualization, writing-reviewing, editing, supervision S.L.S.: conceptualization, writing-reviewing, editing, resources, supervision, funding acquisition, project administration R.J.R.: conceptualization, methodology, validation, formal analysis, writing-reviewing, editing, resources, supervision, funding acquisition, project administrationAll authors reviewed the manuscript.

Declarations

Competing interests
The authors declare no competing interests.

Additional information
Supplementary Information The online version contains supplementary material available at https://doi.org/10.1038/s41598-024-83114-y.

Correspondence and requests for materials should be addressed to R.J.R.

Reprints and permissions information is available at www.nature.com/reprints.

Publisher's note Springer Nature remains neutral with regard to jurisdictional claims in published maps and institutional affiliations.